CAVITY MODE RELATED WIRE BREAKING OF THE SPS WIRE SCANNERS AND LOSS MEASUREMENTS OF WIRE MATERIALS

F. Caspers, B. Dehning, E. Jensen, J. Koopman, J.F. Malo, CERN, Geneva, Switzerland
F. Roncarolo, CERN/University of Lausanne, Switzerland

Abstract

During the SPS high intensity run 2002 with LHC type beam, the breaking of several of the carbon wires in the wire scanners has been observed in their parking position. The observation of large changes in the wire resistivity and thermionic electron emission clearly indicated strong RF heating that was depending on the bunch length. A subsequent analysis in the laboratory, simulating the beam by two probe antennas or by a powered stretched wire, showed two main problems:
i) the housing of the wire scanner acts as a cavity with a mode spectrum starting around 350 MHz and high impedance values around 700 MHz;
ii) the carbon wire used so far appears to be an excellent RF absorber and thus dissipates a significant part of the beam-induced power.
Different wire materials are compared with the classical cavity mode technique for the determination of the complex permittivity in the range of 2–4 GHz. As a resonator a rectangular TE_{01n} type device is utilized.

WIRES HEATING IN THE SPS TUNNEL

During the two last Machine Development periods in the SPS 2002 run, several wires were found broken. Such breaking can be typically related to the wire heating due to some energy deposition by the traversing protons on the wire. Dedicated electronics has been installed in order to have an indication of the wires heating during the LHC type beam injection and ramp in the SPS. In particular a constant current was supplied to the wire and the voltage drop across it was fed to a digital scope together with the difference between the input and output currents. The differential current ($I_{out} - I_{in}$) grow up is due to the wire heating and consequent emission of electrons for thermionic effect. Fig. 1 shows such voltage and differential current evolutions during the SPS cycle with LHC type beam. No scans were performed along this cycle. It is thus evident that the wire heating does not depend on the direct wire-beam interaction. In particular it is possible to relate the wire heating to the beam intensity (two batches of 72 bunches with $1.1 \cdot 10^{11}$ p/bunch injected in this case) and to the bunch length which is decreasing along the beam ramp to 450 GeV.

The measurements described in the previous section clearly revealed that the bunch length shortening causes a larger wire heating than the beam intensity. Such observations lead the study of possible RF coupling effects between the wire scanner wires and the proton beam travelling inside the wire scanner tank which is acting as a cavity.

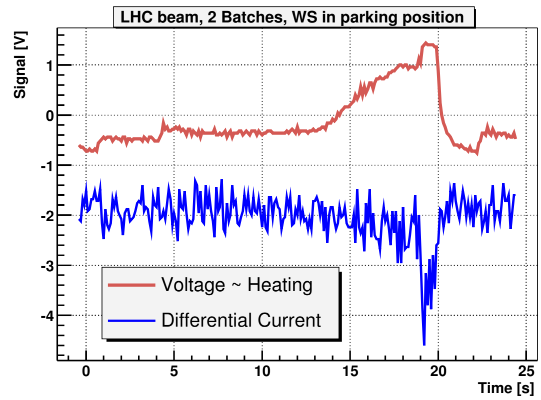

Figure 1: Wire heating due to the LHC beam injection in the SPS (No scan, wire in parking position). The beam energy ramp/bunch length decreasing begin t=11 s.

The proton beam circulating in the ring has a frequency spectrum which mainly depends on the bunching structure (bunch length, bunch spacing). The build up of standing waves resonating inside the tank depends on the geometry and the tank materials. If one or more of the modes matches a beam spectral line, a rather large amount of RF power can be transmitted from the beam to the wires. These hypotheses have been investigated through dedicated laboratory measurements.

LABORATORY MEASUREMENTS

A spare SPS wire scanner tank has been equipped in the laboratory with two probe antennas connected to a Vector Network Analyzer (VNA) in order to simulate the RF modes in the beam spectrum frequency.

Beam-Wire coupling

Two connections to the ends of the wires of the wire scanner are used during normal operation to check the wire integrity (measuring the resistance) or to detect the secondary emission signal. In the laboratory they were applied to estimate the proton beam-wire coupling while simulating the beam with a stretched wire. A $0°/180°$ RF signal combiner circuit has been used to measure the differential signal at the wire ends. One port of the VNA has been connected to one end of the stretched wire, the other one at the combiner output giving the differential signal. Fig. 2 is well describing the effect. The plot gives the S_{21} signal together with the differential signal on the wire scanner wire. Where the frequency peak of the transmitted signal matches a peak of the differential signal, the power present in the cavity can be absorbed by the wire. Different config-

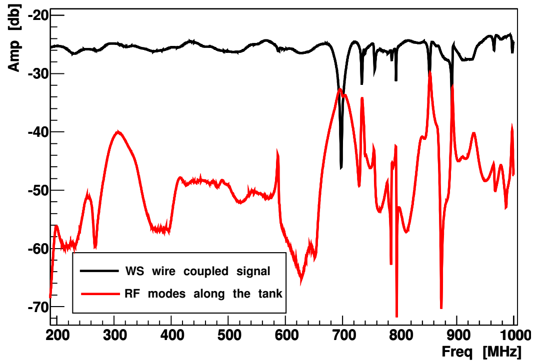

Figure 2: Beam-Wire Scanner coupling

urations have been set up in order to better understand the phenomenon:

1. none of the wires mounted on the forks, without ferrite tiles inserted,
2. one copper and one carbon wires mounted and kept in the parking position, without ferrite tiles,
3. two carbon wires mounted and kept in the parking position, without ferrite tiles,
4. two carbon wires mounted, the horizontal wire kept in the parking position and the vertical wire in proximity of the beam position, without ferrite tiles,
5. two carbon wires mounted, the horizontal wire kept in the proximity of the beam position and the vertical wire in the parking position, without ferrite tiles,
6. none of the wires mounted, nine ferrite tiles inserted in the tank,
7. one carbon wire mounted, nine ferrite tiles inserted in the tank,
8. two carbon wire mounted, nine ferrite tiles inserted in the tank.

For each measurement the Q factor has been evaluated by mean of the VNA, zooming in the resonance interval. For each resonance the antenna-probes position has been adjusted in order to reach the condition of weak coupling (S_{11} and S_{22} signals minimized to $< .5$ dB) thus allowing the evaluation of the unloaded Q. Fig. 3 shows two of the recorded signals, one with no wires mounted and no ferrite tiles inserted and one with no wires installed and nine ferrite tiles inserted. Fig. 4 summarizes all the quality factors as function of frequency, for all the measurement configurations. The RF modes damping by inserting the ferrite tiles is evident and suggested such configuration to reduce the power absorbed by the wire scanners wires. The ferrite type is TT2-111R (from Transtech, Maryland, USA) and its properties can be found in [2].

WIRE MATERIALS STUDIES

The classical cavity mode technique has been used for the determination of the complex permittivity of different wires in the range from 2–4 GHz. As a resonator a rectangular TE_{01n} type device is utilized. Different materials

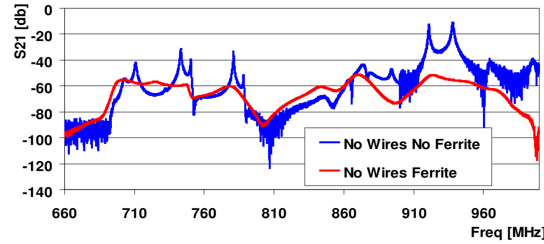

Figure 3: Transmitted signal from one end of the tank to the other using the antenna-probes method

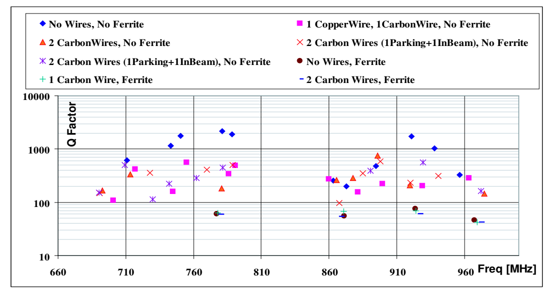

Figure 4: Unloaded Q factors for all the measurements setups as function of frequency

such as silicon carbide (SiC), carbon and quartz fibers were examined. SiC fibers are an interesting alternative to carbon fibers and their properties had to be investigated, since SiC bulk material is often used as a microwave absorber.

The complex permeability can be expressed as

$$\vec{\epsilon} = \epsilon_0 \vec{\epsilon_r} = \epsilon_0 \left(\epsilon_r^{'} - j\epsilon_r^{''}\right) \tag{1}$$

from where the loss factor can be defined:

$$\tan \delta_\epsilon = \frac{\epsilon_r^{''}}{\epsilon_r^{'}} \tag{2}$$

In the test cavity there are locations, in which either the electric or the magnetic field vanishes. If one puts a sufficiently small sample, which does not disturb the field, in these locations only the magnetic or electric properties of the cavity are influenced by the sample. In both cases the resonance frequency f_r and the quality factor Q are changed. $\epsilon_r^{''}$, $\epsilon_r^{'}$ and $\tan \delta_\epsilon$ respectively can be found from these changes. [1] provides:

$$\frac{\Delta \vec{f_r}}{\vec{f_r}} = -\frac{\Delta \vec{W}}{\vec{W}} \tag{3}$$

The variables in this equation are complex. $\mathrm{Im}(\vec{f_r})$ and $\mathrm{Im}(\vec{W})$ describe the losses in the empty cavity, and given the high Q they will be neglected in the following. If the sample is non-magnetic and positioned in a zero-magnetic-field region, then $\vec{W}$ and $\Delta\vec{W}$ in Eq. (3) are only calculated from the electrical fields:

$$\begin{aligned} \frac{\Delta \vec{f_r}}{\vec{f_r}} &= \frac{\vec{f_{r_s}} - \vec{f_{r_e}}}{\vec{f_{r_e}}} \\ &= \frac{-\epsilon_0 \int_{v_s} (\vec{\epsilon_r} - 1) E(x, \vec{y}, z)_e E(x, \vec{y}, z)_s * \mathrm{dV}}{2\epsilon_0 \int_{v_r} E_e^2 \, \mathrm{dV}} \end{aligned} \tag{4}$$

The subscripts e and s indicate the empty cavity and the cavity with sample, whilst V_s and V_r are the volumes of the sample and of the resonator. When the electric field is tangential to the surface of the sample and the sample ends on the resonator walls, then the internal field equals the external field:

$$E_e = E_s \tag{5}$$

Given a small volume of the sample:

$$\vec{E}_e(x,y,z) = \vec{E}_{e0} \tag{6}$$

and can be pulled out from the integrals of Eq. (4). The imaginary part of the resonant frequency shift is related to the change in quality factor:

$$\mathrm{Im}(\Delta\vec{f}_r) = \Delta f_r^{''} = \frac{f_r}{2}\left[\frac{1}{Q_{L_s}} - \frac{1}{Q_{L_e}}\right] \tag{7}$$

Eq. (4) to Eq. (7) lead to the evaluation of the real and imaginary part of the dielectric constant:

$$\epsilon_r^{'} = 1 - \frac{f_{r_s} - f_{r_e}}{f_{r_e}}\frac{V_r}{2V_s} \tag{8}$$

$$\epsilon_r^{''} = \left[\frac{Q_{L_e}}{Q_{L_s}} - 1\right]\frac{1}{Q_{L_e}}\frac{V_r}{4V_s} \tag{9}$$

and therefore to the characteristic loss factor as defined in Eq. (2). $\epsilon_r^{''}$ can also be deduced from the material conductivity σ and the resonant frequency f according to:

$$\sigma = \omega\epsilon^{''} = 2\pi f\epsilon^{''} = 2\pi f\epsilon_0\epsilon_r^{''} \tag{10}$$

Experimental Results

In the laboratory fibers of three different materials were considered: Carbon, Silicon Carbide and Quartz. Fig. 5 shows the measurements results as signal intensity versus frequency, around one of the resonating modes with maximum electric field at the sample location. The plot qualitatively proves the RF power absorption of Carbon, and the non-absorption of Silicon Carbide and Quartz. Fig. 5 also includes the results of a numeric simulation and measurement concerning the SiC material which is presently considered as a suitable RF absorber for the Compact Linear Collider (CLIC). A pyramid shaped piece of such material was inserted in the resonator at the same location where the wire scanner wires were placed. The fact that this material is absorbing RF power as shown by the simulation and by the measurements, proved that this is a SiC compound different from the one used for the wire scanners wires.

The insertion of one carbon fiber (d=36 μm) is reducing the signal amplitude to a level where the mode frequency is not well defined since the resonance curve is strongly asymmetric. Therefore, for this material, we could not apply Eq. (8). The imaginary part of the dielectric constant was evaluated both from Eq. (9) and Eq. (10). The insertion of 500 SiC fibers (d=15 μm) allowed the evaluation of both the real and imaginary part of the dielectric constant by mean of Eq. (8) and Eq. (9). The results for the TE_{103} are summarized in the table below, together with the available data for the CLIC SiC bulk material [3]. Being Quartz a weakly absorbing material, in order to evaluate ϵ' and ϵ'' one should insert a large number of fibers as it has been done for SiC. However not enough Quartz material was available.

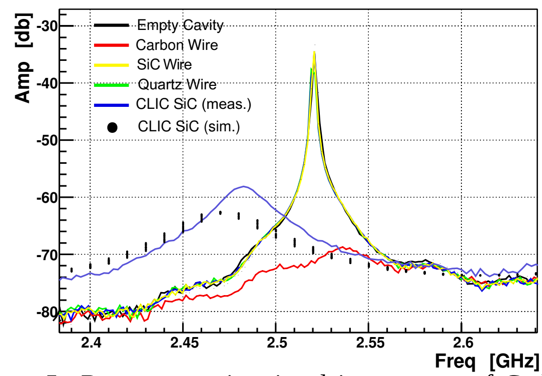

Figure 5: Resonant cavity signal in presence of Carbon, Silicon Carbide and Quartz

	ϵ_r'	ϵ_r''
C		$2.30 \pm 0.05 \cdot 10^5$
SiC	10.790 ± 0.016	2.158 ± 0.005
SiC (CLIC)	14.4	6.6

Table 1: Real and imaginary part of the dielectric constant for the TE_{103} mode, at 2.5 GHz.

CONCLUSIONS

The laboratory measurements investigated the RF coupling nature responsible for the wire breaking in the SPS wire scanners. The wire scanners tanks proved to act as resonant RF cavities in the beam spectrum frequency range. As a cure for the wire heating due to the beam-wire coupling, the SPS wire scanner tanks have been equipped with low outgassing ferrite tiles in order to damp the resonance modes. Carbon, used in the SPS until 2003, provided evidence of RF absorption properties. Therefore the wire material of few monitors were changed from carbon to silicon carbide, which has been characterized as a weakly absorbing material, and will be tested during the 2003 SPS run.

ACKNOWLEDGMENTS

We thank G. Burtin for the useful discussions.

REFERENCES

[1] E.Nyfors, P.Vainikainem, *Industrial microwave sensors*, Artech House (1989)

[2] E.Campisi, R.Doolittle, *Proceedings of the Workshop on Microwave-Absorbing Materials for Accelerators (p.169)*, Newport News, Virginia, US (1993)

[3] M.Luong, *Private communication*, CEA-CEN-Saclay, 91191 Gif sur Yvette, France